Journal of Applied Polymer Science

Influence of a graphene oxide additive and the conditions of membrane formation on the morphology and separative properties of poly(vinylidene fluoride) membranes

Beata Fryczkowska, Marta Sieradzka, Ewa Sarna, Ryszard Fryczkowski, Jarosław Janicki
Institute of Textile Engineering and Polymer Materials, University of Bielsko-Biala, Willowa 2, 43-309 Bielsko-Biala, Poland
Correspondence to: B. Fryczkowska (E-mail: bfryczkowska@ath.bielsko.pl)

ABSTRACT: In this article, we present our study of the influence of a graphene oxide (GO) additive and the method of preparation on the properties of membranes. Poly(vinylidene fluoride) (PVDF)/GO membranes were obtained by an inverse phase method, which was conducted by two different methods. The first one was based on solvent evaporation, and the second method was a coagulation bath in distilled water. Our studies clearly showed that the introduction of the GO nanoadditive into the polymer membrane matrix played a major role in the pore process formation, and it also contributed to the reduction of the contact angle, and this led to an improvement in the hydrophilic properties of the obtained membranes. Furthermore, the PVDF/GO membrane preparation process had a direct influence on the thickness and porosity. Both of these factors had a direct influence on the transport properties of the membrane. © 2015 Wiley Periodicals, Inc. J. Appl. Polym. Sci. **2015**, *132*, 42789.

KEYWORDS: graphene and fullerenes; membranes; morphology; nanotubes; property; structure relations

Received 18 February 2015; accepted 30 July 2015
DOI: 10.1002/app.42789

INTRODUCTION

Membrane processes were developed in the 20th century, and until now, there has still been wide interest in those techniques. The competitiveness of membrane techniques in comparison to other separation methods are related to the process of energy consumption savings, the regeneration of raw materials, and the ease of scaling up the process.[1] Because of these advantages, membrane processes have found numerous industrial applications in environmental protection and the food, chemical, pharmaceutical, textile, and petrochemical industries.[2–5] Nowadays, membranes are produced on an industrial scale mainly from organic polymers. Among them, poly(vinylidene fluoride) (PVDF) is worth distinguishing because of its high chemical and mechanical resistance, thermal stability, and antioxidation activity and good membrane-forming properties.[6–8] PVDF enables the production of membranes for ultrafiltration, microfiltration, and pervaporation.[1,9,10]

An application of the PVDF in numerous membrane techniques causes that the obtained membranes should possess diverse properties.[11] The series of performed investigations confirmed that there were a lot of factors that, during membrane formation, had an influence on the morphology and permeability. It has been proven that parameters such as the type of solvent, temperature, time, and composition of the coagulation bath, evaporation time, and organic or inorganic additives have a crucial influence on the morphology of the obtained membranes.[12–15] Wang *et al.*[15] investigated the effects of the solvent and solvent mixtures on membrane morphology, physicochemical properties, and permeability. The results show that the application of various solvents and their mixtures cause the production of various types of pores. On the cross sections of the obtained membranes, three types of pores could be distinguished: (1) short fingerlike cavities with the spongelike structures, (2) interconnected macrovoids, and (3) the spongelike structure only.

Despite its almost ideal chemical, mechanical, and thermal properties, PVDF also possesses disadvantages that limit the widespread industrial production of membranes. The hydrophobic characteristics of this polymer have a crucial influence on the reduction of the permeability and subsequently increase the probability of membrane fouling.[16] Those limitations can be eliminated through the use of additives that increase the hydrophilicity. The introduction of oxide nanoparticles, such as TiO_2, Al_2O_3, Fe_3O_4, or SiO_2, and carbon nanotubes into the polymer matrix subsequently improves the hydrophilic properties of the membrane, and it also has a positive influence on its strength and permeability.[17–22] In recent years, investigations have revealed that similar effects could be expected after graphene oxide (GO) was introduced into the polymer matrix.[14,23]

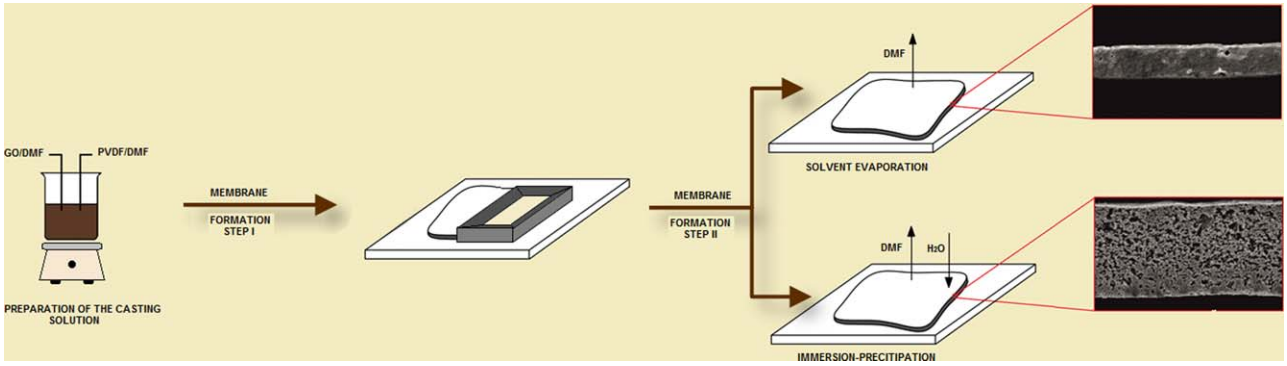

Figure 1. Schematic illustration of the PVDF/GO membrane preparation process. [Color figure can be viewed in the online issue, which is available at wileyonlinelibrary.com.]

Because of the presence of oxygen-containing functional groups (e.g., hydroxyl, epoxide, carbonyl, and carboxyl groups), GO itself qualifies perfectly as an additive to form PVDF membranes and improve their hydrophilic characteristics.[24] Moreover, the application of GO may also have a positive influence on the mechanical and separation performance of the membranes.[25] The positive effects of a GO additive on PVDF membranes were observed by Wang *et al.*,[25] who obtained these kinds of membranes with the immersion phase-inversion process. Their studies showed that even a small GO addition (0.20 wt %) improved the structure and properties of the membranes. Compared with the pure PVDF membrane, the contact angle of the PVDF/GO membranes decreased from 79.2 to 60.7°. The investigations of Zhao *et al.*[16] showed that the addition of GO to PVDF membranes resulted in better antifouling properties and higher pure water and permeation fluxes. The authors suggest that this effect was caused by the surface hydrophilicity and smoother surface with a higher efficient filtration area. An *et al.*[26] observed a strong influence on the formation of β-phase PVDF when GO was added. The authors described a preparation method for GO/PVDF films through which the β-phase content increased significantly and the dielectric constant improved significantly with a low dielectric loss.

In this study, we present the results of a study illustrating the influence of selected factors on the morphology and physicochemical and separation properties of PVDF membranes. As a solvent for the polymer in question, *N,N*-dimethylformamide (DMF) was used because it is a good solvent for PVDF, and it allows the creation of stable and homogeneous dispersions with GO.[27] Membranes were obtained by a phase-inversion method by two different techniques. The first was the evaporation of the solvent at a high temperature without a coagulation bath. The second method was the preparation of the membranes by the immersion–precipitation process (a so-called wet process), the most popular membrane preparation method.

EXPERIMENTAL

Materials

PVDF was purchased from Solvay (Solev 1008). GO was obtained from a graphite powder (<20 μm) supplied by Sigma-Aldrich. The other reagents, including $NaNO_3$, 98% H_2SO_4, $KMnO_4$, 30% H_2O_2, and DMF, were purchased from Avantor Performance Materials Poland S.A.

Preparation of GO

GO was obtained by the modified Hummers method.[28] An amount of 2 g of graphite powder were added to a mixture containing 1 g of $NaNO_3$ and 46 cm^3 of H_2SO_4. The obtained suspension was stirred for 30 min in an ice bath. Then, by portions, 6 g of $KMnO_4$ was added in such a way that the temperature did not exceed 20°C. After 5 min, the contents of the beaker were warmed to 35°C and stirred for 4 h. This was followed by the addition of 92 cm^3 of distilled water. To remove the nonreacted traces of $KMnO_4$, 80 cm^3 of warm distilled water (60°C) and 50 cm^3 of a 3% aqueous solution of H_2O_2 were added. The obtained GO was centrifuged and rinsed with distilled water several times until a pH of 7 was achieved. After drying at 60°C, the brown GO precipitate was obtained. An ultrasonic bath was used to redisperse the GO powder in DMF.

PVDF/GO Membrane Preparation

PVDF/GO membranes were obtained by the phase-inversion method. PVDF was dissolved in DMF at a temperature of 70°C. To the obtained 20 wt % casting solution, a proper amount of a permanent dispersion of GO/DMF was added, and this mixture was stirred with simultaneous sonication for 4 h until it became a homogeneous mixture containing 0; 0.1; 0.5; 1.0, or 2.0% GO in relation to the PVDF mass. The prepared casting solutions were left to release air bubbles for 24 h. On the glass plates, membranes were formed by the use of a casting knife with a knife gap set at 300 μm. One part of the membranes was obtained by the solvent evaporation method at 70°C (technique 1). The evaporation process was performed over several hours; subsequently, the membranes were immersed in distilled water and left for further characterization. The rest of the membranes were obtained by the wet process. The glass plate was allowed to sit at room temperature for 30 s and was then immersed into a coagulation bath (distilled water at 25°C; technique 2). The wet membranes were stored in distilled water for subsequent analysis. The methods through which the PVDF/GO membranes were obtained are shown in Figure 1.

Table I. Membrane Properties Obtained with Two Separate Techniques and Various Contents of GO

Method for obtaining the membranes	Sample name	GO content (%)	Contact angle (°)	Porosity (%)	Mean pore size (μm)	Thickness (μm)
Solvent evaporation (technique 1)	M-1	0	97.7 ± 0.8	10.4 ± 0.8	0.065 ± 0.011	9.0 ± 1.6
	M-2	0.1	91.3 ± 0.9	14.3 ± 0.3	0.073 ± 0.010	25.7 ± 2.0
	M-3	0.5	90.8 ± 1.1	16.5 ± 0.6	0.115 ± 0.009	27.4 ± 1.7
	M-4	1.0	87.7 ± 1.3	3.6 ± 0.1	0.057 ± 0.013	19.5 ± 2.1
	M-5	2.0	64.3 ± 0.4	9.4 ± 0.2	0.074 ± 0.022	20.2 ± 1.0
Immersion–precipitation process (technique 2)	M-6	0	61.0 ± 1.0	24.9 ± 1.1	0.223 ± 0.016	68.2 ± 2.5
	M-7	0.1	59.7 ± 0.8	43.2 ± 0.9	0.256 ± 0.022	73.9 ± 3.2
	M-8	0.5	48.0 ± 1.1	35.3 ± 0.4	0.295 ± 0.027	84.0 ± 2.2
	M-9	1.0	45.0 ± 1.1	44.3 ± 1.5	0.307 ± 0.012	63.8 ± 2.5
	M-10	2.0	44.0 ± 1.3	21.8 ± 0.5	0.176 ± 0.018	45.7 ± 2.9

Investigation Methods

The prepared samples of GO were characterized by X-ray diffraction, thermogravimetric analysis, and Fourier transform infrared spectroscopy.

X-ray diffraction investigations were carried out with a URD 63 Seifert diffractometer. Cu Kα radiation was used at 40 kV and 30 mA. Monochromatization of the beam was obtained by means of a nickel filter and a pulse-height analyzer. A scintillation counter was used as a detector. Investigations were performed in a range of angles of 4–40° with a step of 0.05°. Each of the diffraction curves were corrected for polarization, the Lorentz factor, and incoherent scattering.

The thermal properties of the samples were characterized with a thermogravimeter (TGA Q500 V20.10 Build 36), and all of the measurements were carried out over a temperature range of 30–850°C with a 10°C/min heating rate under nitrogen gas (flow rate = 60 mL/min).

Fourier transform infrared analysis measurements were taken with a Magna-IR 860 spectrophotometer supplied by Thermo-Nicolet with the following parameters: resolution = 4 cm^{-1}, number of scans = 32, and measurement range = 4000–400 cm^{-1}.

The hydrophilic characteristics of the obtained membranes were determined by the value of the contact angle measured by a goniometer (type PG-1, FIBRO System AB). On the surface of the prepared sample, we put a drop of distilled water from a syringe. The angle between the membrane flat surface and the tangent plane to the drop surface was read. Each of the samples was measured 10 times, and the average value is shown in Table I.

The membrane porosity (ε; %) was defined as the pore volume divided by the total volume of the membrane. The pore volume was determine by the gravimetric method with the following formula:[9]

$$\varepsilon = \frac{(w_1 - w_2)/dw}{(w_1 - w_2)/d_w + w_2/d_p} \times 100\% \quad (1)$$

where w_1 is the wet membrane weight (g), w_2 is the dry membrane weight (g), d_w is the distilled water density (0.998 g/cm^3), and d_p is the polymer density (1.78 g/cm^3).

The mean pore size (r_m) was determined by the Guerout–Elford–Ferry equation [eq. (2)] on the basis of the pure water flux and the porosity data:[29]

$$r_m = \sqrt{\frac{(2.9 - 1.75\varepsilon)8\eta l Q}{\varepsilon A \Delta P}} \quad (2)$$

where η is the water viscosity (8.9×10^{-4} Pa s), l is the membrane thickness (m), Q is the volume of permeated pure water per unit of time (m^3/s), and ΔP is the operational pressure (0.1 MPa).

The thickness was measured by a thickness gauge (Elmetron MG-401). The tested samples were subjected to 10 measurements, and the average value is presented in Table I.

The surface and cross-sectional structure of the membranes were examined with a scanning electron microscope (JSM.5500 LV JEOL). Cross-sectional samples were prepared by the fracturing of the membranes after cooling in liquid nitrogen.

The flux measurements were performed with the use of a dialysis capsule (QuixSep dialyzer, MFPI). To the capsule, 4 cm^3 of methylene blue solution was introduced. The membrane in question was put on an apparatus base filled with dye. The capsule was closed hermetically and immersed immediately in a beaker filled with 400 cm^3 of distilled water. The whole thing was stirred with a magnetic stirrer; after 5 min, the sample was taken out of the beaker and examined with an ultraviolet–visible spectrophotometer (PerkinElmer Lambda 35 ultraviolet–visible spectrometer). These operations were repeated several times. The results are presented later in Figure 7 as the transport properties related to the concentration of dye over time.

The membrane permeation performance was measured by ultrafiltration experimental equipment. The membrane effective area was 34.2 cm^2. The new membranes were prepressed at 2 bar for 1 h to compact membranes, and then, the pure water flux was measured at 1 bar with the following equation:

$$J_W = \frac{Q}{At} \quad (3)$$

where J_W is the water flux (L/m^2 h), Q is the volume of the permeate water (L), A is the effective membrane area (m^2), and t is the permeation time (h).

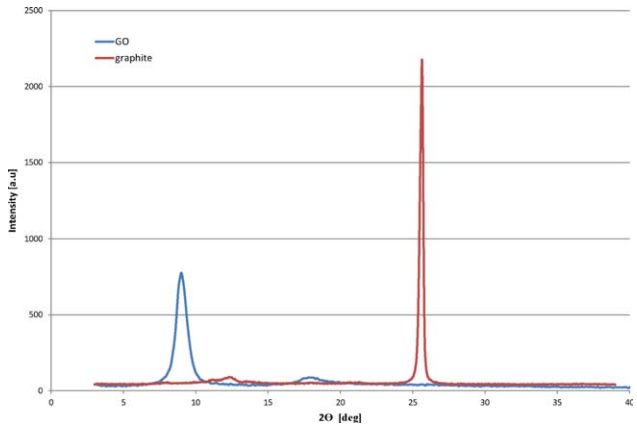

Figure 2. X-ray diffraction patterns of the pristine graphite and GO. [Color figure can be viewed in the online issue, which is available at wileyonlinelibrary.com.]

RESULTS AND DISCUSSION

Characterization of GO

The obtained GO before introduction into the polymer matrix was characterized by X-ray diffraction, thermogravimetric analysis, and Fourier transform infrared spectroscopy.

Figure 2 shows the X-ray diffraction patterns of the original graphite and graphite oxide. For the pristine graphite, a strong sharp peak at a 2θ of 25.6°, corresponding to an interlayer spacing of 0.34 nm, was observed. After oxidation, this peak disappeared almost completely, and a new diffraction reflection centered at $2\theta = 9°$ arose. On the basis our of previous research, we determined that this peak was the typical diffraction peak of GO.[30] In this case, the interlayer distance increased up to 0.80 nm because of the incorporation of the oxygen-containing functional groups or absorbed moisture.

Thermogravimetric analysis curves of the pristine graphite and graphite oxide are shown in Figure 3. As we expected in the case of pure graphite, almost no mass decrease was observed with a temperature increase. Strictly, the opposite effect was observed on the GO curve. With temperature growth, sample mass loss occurred in three stages. In the first stage, at temperatures below 100°C, the GO sample was reduced by about 6.4% of its initial mass. This phenomenon was related to the release of intercalated water molecules between the GO sheets. The next stage occurred above 100°C, where the mass reduction was about 36.4%. This stage was associated with the decomposition of less stable oxygen-containing functional groups on the GO sheets.[31] The third decomposition stage resulted from the removal of more stable functional groups and occurred above 400°C with a 46.5% weight loss.

The obtained samples were also investigated with Fourier transform infrared spectroscopy. The results are presented in Figure 4. On the GO spectrum, there were visible bands characteristic for oxygen-containing functional groups, including C═O stretching vibrations at 1740 cm^{-1}, C─OH stretching vibrations at 1215 cm^{-1}, and C>O vibrations at 1049 and 984 cm^{-1}, in comparison to the graphite spectrum. There was also a band at 1628 cm^{-1}, which corresponded with the aromatic C═C ring stretching.[32,33] On the spectrum, GO was present in a wide peak from 2900 to 3600 cm^{-1}. This peak was related to the vibrations of O─H bonds in the hydroxyl groups. The content of this group corresponded to the hydrophilic properties of GO[31] and ensured the formation of stable GO dispersions in water.

Characterization of the Membranes

There are a lot of formation methods in the literature for PVDF membranes. However, the phase-inversion method is regarded as the most commercial because of its simplicity and economical aspects.[12] As already indicated in this article, there are two ways of preparing membranes by this technique. One of them is solvent evaporation from polymer films under increased temperature conditions. The other is a classic method based on thin-film formation from a solvent–polymer solution followed by a coagulation bath with a nonsolvent. To determine the influence of the membrane-formation conditions on its properties and morphology, the following measurements were performed: contact angle, thickness, porosity, mean pore size, morphologies of the cross section and surface of membrane, transport of substances across the membrane, and pure water flux.

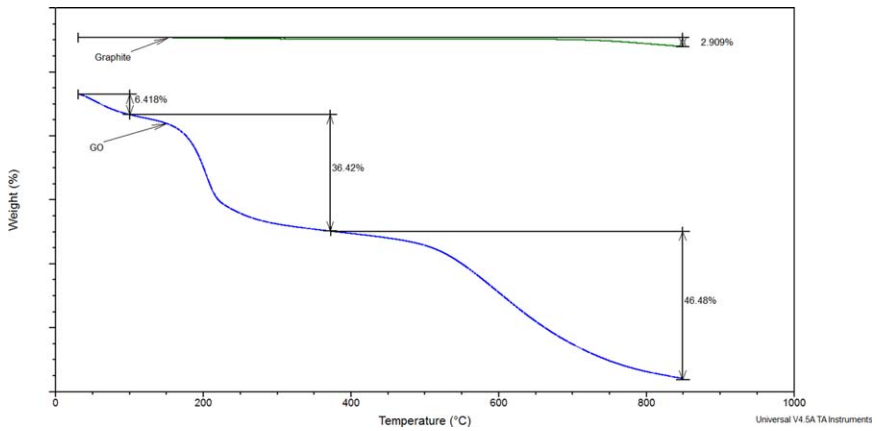

Figure 3. Thermogravimetric analysis curves of the pristine graphite and GO. [Color figure can be viewed in the online issue, which is available at wileyonlinelibrary.com.]

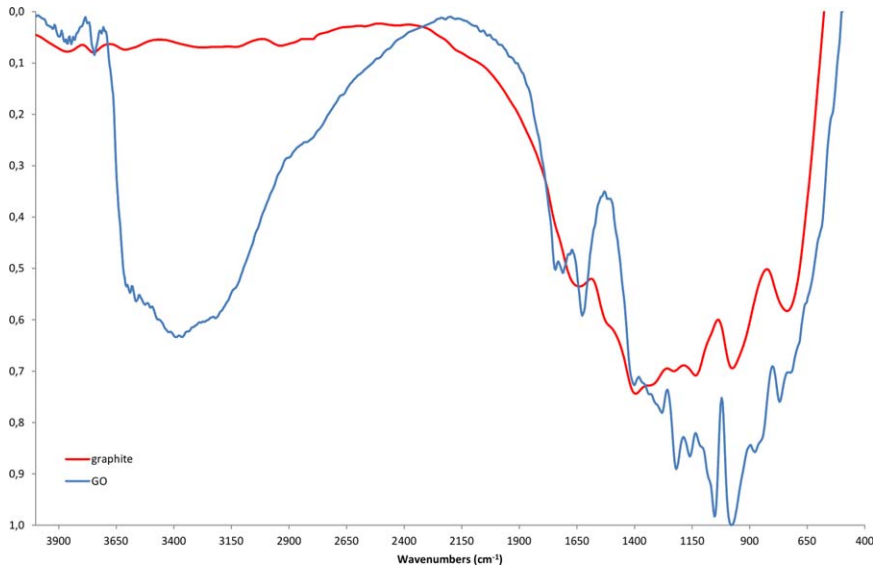

Figure 4. Fourier transform infrared spectra of the pristine graphite and GO. [Color figure can be viewed in the online issue, which is available at wileyonlinelibrary.com.]

The contact angle is an important parameter that enables one to describe the hydrophilic characteristics membranes. The lower the contact angle value is, the more hydrophilic the surface is. As shown by the data presented in Table I, there were two factors that had an influence on the hydrophilic characteristics of the obtained membrane: the method of their formation and the presence of additive in the form of GO. With increasing in total GO content in the polymer matrix, the contact angle decreased independently of the technique of the membrane formation. This phenomenon was certainly related to the presence of the additive with numerous oxygen-containing functional groups; this improved the hydrophilic characteristics of the membrane. As mentioned, the presence of this group was confirmed by Fourier transform infrared spectroscopy (Figure 4) with a wide peak from 2900 to 3600 cm^{-1}. This led us to conclude that the introduction of a proper amount of GO effectively decreased the contact angle and simultaneously improved the hydrophilicity of the membrane surface.

Comparing the values of the contact angles of the membrane obtained by technique 1 to the values of those obtained by technique 2, we observed the membranes with better hydrophilic properties coagulated in the distilled water (technique 2). This phenomenon may have been related to the hydrophilic characteristics of GO. During membrane formation through an immersion–precipitation process, GO migrated to the surface of the membrane; because of the hydrophilic nature of GO and its affinity to water, this occurred spontaneously.[24] This, in turn, revealed that even a 0.5% GO concentration was sufficient to improve the membrane hydrophilicity, and a further increase to 2% had a negligible influence on the contact angle value. During long-lasting solvent evaporation (technique 1), the membrane was not immersed in water; that is why GO did not migrate into the surface so easily. This effect may have been responsible for the slight improvement in the membrane hydrophilicity at GO concentrations ranging from 0.1 to 1.0%. When the concentration in the polymer matrix of GO was sufficient, up to 2%, the contact angle decreased rapidly by 33°. Thereby, the membrane was transformed to a hydrophilic membrane.

The processes occurring while the membranes were formed had an influence on the total thickness as well. The results are shown in Figure 5 and Table I. The pure PVDF membrane obtained by technique 2 had a 68.2 ± 2.5 μm thickness, whereas the thickness of the same membrane formed by technique 1 was only 9.0 ± 1.6 μm. GO addition into the polymer matrix in water-coagulated membranes resulted in a higher overall thickness than in the membranes formed by evaporation, although this difference was not so significant. When the GO content was below 1%, the thickness was three times higher in comparison to the membranes obtained by solvent evaporation. For membranes containing 2% GO, the difference was lower; it reached 20.2 ± 1.0 to 45.7 ± 2.9 μm for membranes obtained by technique 1 and 2, respectively.

As shown in the scanning electron microscopy pictures, the morphology of the membranes depended on the selected technique of formation and GO content. The scanning electron microscopy images in Figures 5 and 6 present the cross section and top and bottom surfaces of the membranes obtained with two techniques and differing with GO contents. The images also show the surfaces of six membranes; the rest had similar top and bottom morphologies.

The membranes obtained by solvent evaporation had a symmetric, spongy, and dense structure with fewer pores (M-1 to M-5). Among the polymer films prepared by that technique, the highest porosity membrane had a 0.5% GO content, as presented in M-3 picture. This structure had fine pores that were distributed homogeneously across the whole cross section of the membrane. From Figure 5 and Table I, we concluded that GO addition into the polymer matrix at contents from 0.1 to 0.5% caused the porosity and the mean pore size to increase in comparison to

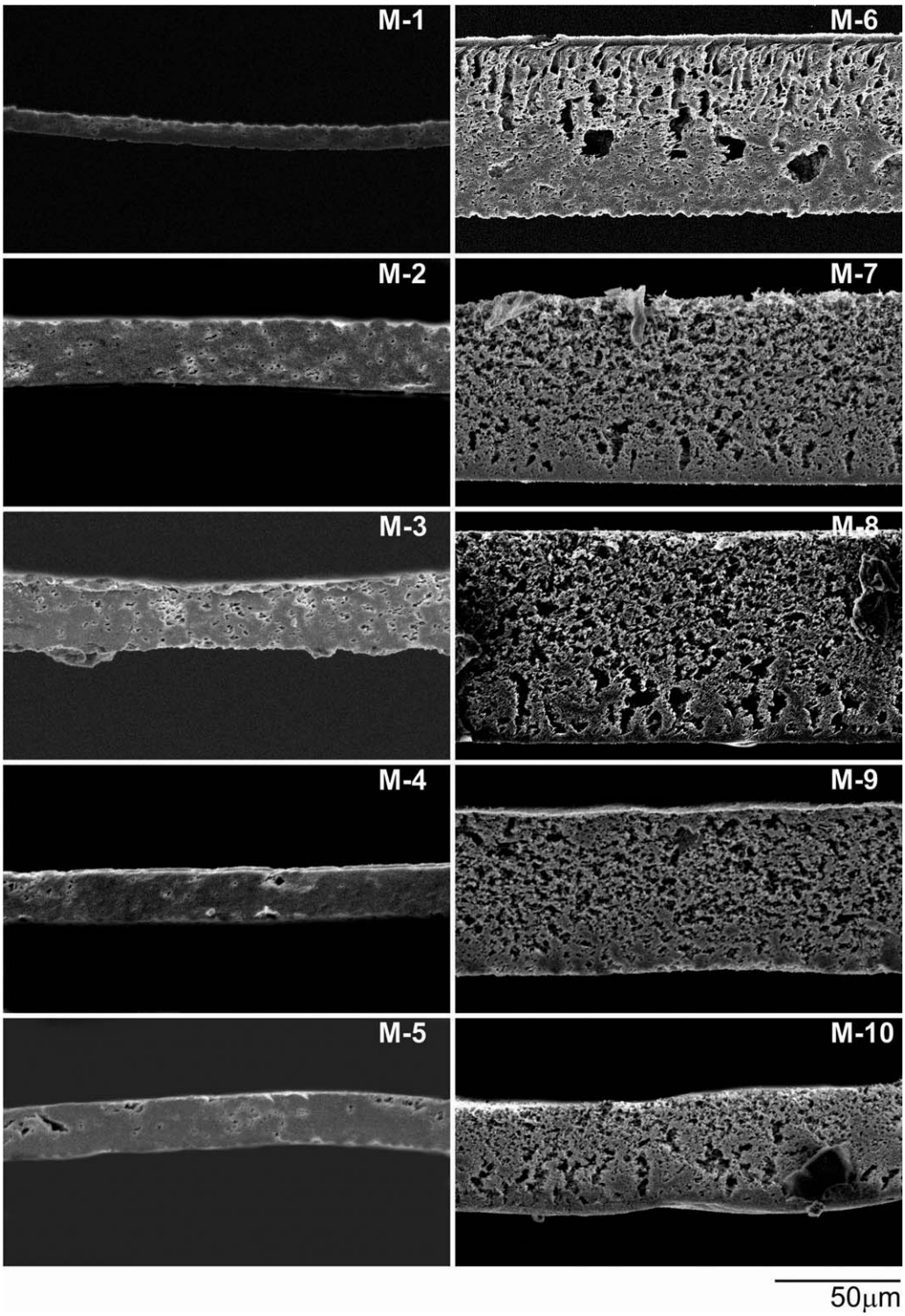

Figure 5. Scanning electron microscopy images of the cross sections of the membranes obtained with technique 1 (M-1 to M-5) and technique 2 (M-6 to M-10).

the pure PVDF membrane. This situation was directly the opposite when the concentration was increased to a level above 1% such as in the case of M-4 and M-5.Then, the membrane became denser and more flat, and on the cross section, there were only macropores visible. Xia and Ni[7] concluded that increasing GO content in the casting solution resulted in viscosity growth, and this slowed down the formation process and, consequently, resulted in a denser structure.

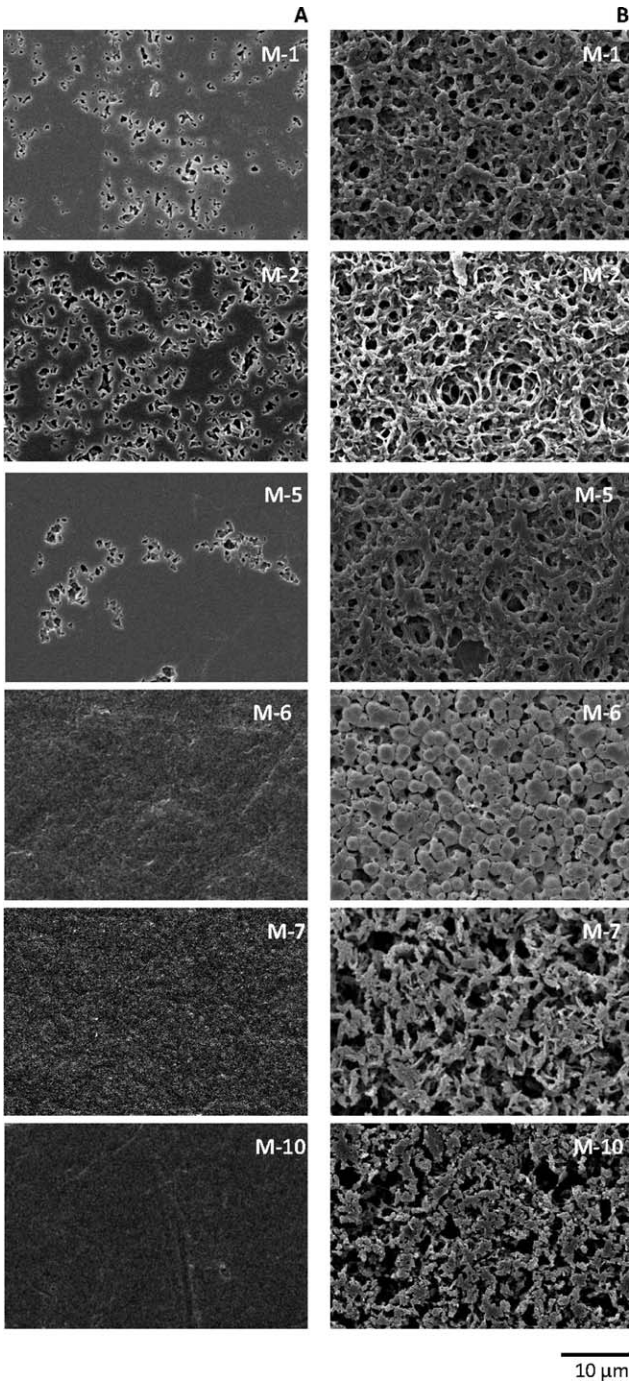

Figure 6. Scanning electron microscopy images of the top and bottom surfaces of the membranes obtained with technique 1 (M-1, M-2, and M-5) and technique 2 (M-6, M-7,and M-10).

An asymmetric structure typical for membranes formed by phase inversion coagulated in water is shown in the pictures for M-6 to M-10 (Figure 5). As shown, GO addition had a substantial influence on the porosity of the films. The pure PVDF membrane had a definitely thicker skin layer and sublayer, which included fingerlike pores and macrovoids. The introduction of 0.1% GO into the polymer membrane matrix caused the skin layer to be thinner, whereas 0.5% GO addition resulted in a skin layer that faded almost completely. This was attributed to the migration of GO particles in the direction of the coagulation bath through the skin layer.[24] Apart from the membrane enrichment, such GO contents favored the formation of a homogeneous pore distribution with regular shapes. We assumed that in case of membrane M-8, closed pores were formed, because as shown by the data in Table I, its porosity was almost 8% lower in comparison to membranes M-7 and M-9. The GO contents increased above 1%; this caused the skin layer to be thicker and denser, but the total membrane thickness decreased. Moreover, in the case when the GO additive was above 2%, the membrane porosity then dropped. During the formation of the film by the so-called wet process, in the first stage, the formation of the thin skin layer occurred, and then, there was the diffusion of the solvent into the membrane structure after its immersion in the coagulation bath. As a result of mass transfer at regions where the polymer concentration was poor, pores were formed, and where the polymer concentration exceeded a certain level, precipitation occurred.[15] The introduction of the hydrophilic GO additive resulted in an increase in the membrane porosity because of acceleration of the mass transfer between the solvent and nonsolvent.[7,16,25] However, when the amount of additive exceeded a certain threshold, the membrane properties were not enhanced. Picture M-10 presents a more flat-sheet and less porous membrane. Because this was similar to the case of membranes formed by technique 1, this could be explained by the casting solution viscosity growth.

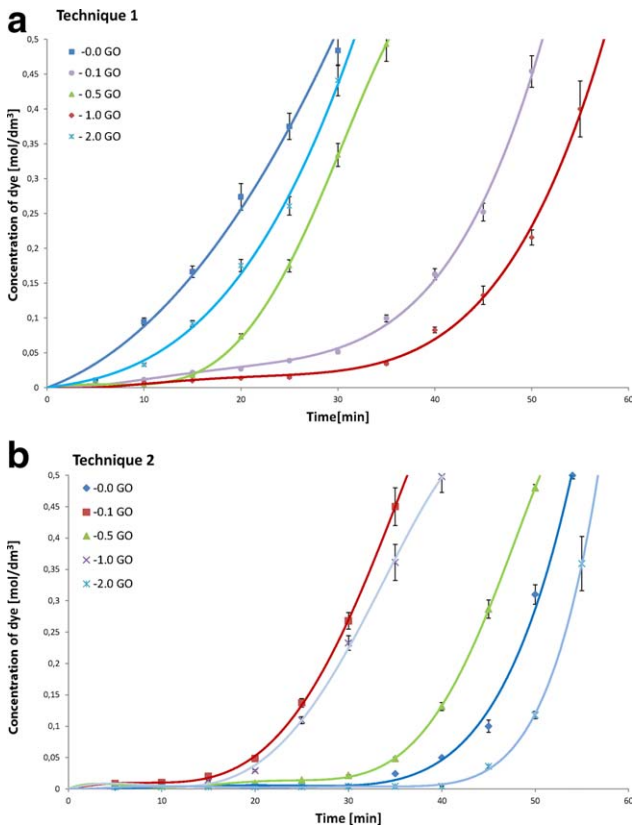

Figure 7. Dye transport through the PVDF/GO membranes obtained with (a) technique 1 and (b) technique 2. [Color figure can be viewed in the online issue, which is available at wileyonlinelibrary.com.]

The top and bottom membranes surfaces owned strictly different structures. The difference could also be seen in the cases of membranes formed by techniques 1 and 2. The top surface was more dense than the bottom surface, which was highly porous, for both the coagulated and evaporated membranes. However, in the case of the evaporated membranes, the surface was studded with single pores, which were not visible on the surface of the coagulated membranes. This disparity was probably sourced in the rate of the skin-layer formation. When the casting solution was immersed in the coagulation bath, polymer precipitation occurred immediately, and then, the nonsolvent diffused into the membrane.[15] In contrast, during the formation of the evaporated membrane, a skin layer was slowly created. On the surface a polymer-poor phase formed, and pores appeared there. Membranes in which the GO contents were 0.1 and 0.5% were characterized by the highest porosity and mean pore size (Table I).

As observed in the scanning electron microscopy images in Figure 6, the bottom surfaces of the membranes were more porous than the top surfaces. This phenomenon occurred for both the evaporated and coagulated membranes. In pure PVDF, the polymer was precipitated as spherulitic structures. The GO additive resulted in the disappearance of those structures, and in their place, interconnected pores formed. Spherulitic structure formation during the phase-inversion process was determined by polymer crystallization despite liquid–liquid demixing.[12,13] The introduction of a GO additive with hydrophilic groups increased the mass transfer rate and resulted in a more porous structure.[9,16]

The formation technique of the PVDF/GO membrane influenced the transport properties as tested by the dialysis capsule. Among films obtained by solvent evaporation, the best transport properties were evident in membranes containing 0 or 2% GO. The pure PVDF membrane was the thinnest and was denser, and that was why it was supposed to be characterized by diffusive transport; this allowed the dye particles to be transported through the polymer chains. The membrane containing 2% GO showed similar behavior. Membrane M-3 (0.5% GO) possessed comparable properties and were characterized by a relatively high number of pores; this enabled easy transport of the applied substance. Although the membrane enriched with 0.1% GO additive had a porosity at the same level as the M-3 membrane, dye transport took place at a definitely lower level. Curve M-2 [Figure 7(a)] shows that transport through the membrane did not begin immediately but about 30 min after the experiment started. This phenomenon was probably related to the relatively small but numerous pores of membrane M-2. When the dye was transported through the structure of the membrane, it was adsorbed in the pores, and after its concentration increased, desorption could occur. The slowest dye transport was observed in the case of the membrane with the lowest porosity where the GO content was 1%.

For membranes obtained by the wet process, the run of dye transport was analogous to the membrane porosity (Figure 5). This observation confirmed that the membranes with contents of GO of 0.1 and 1.0% had the best transport properties. As

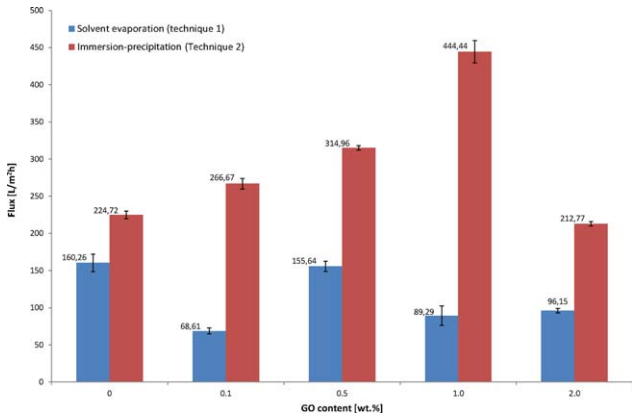

Figure 8. Pure water flux of the obtained membranes with various contents of GO. [Color figure can be viewed in the online issue, which is available at wileyonlinelibrary.com.]

stated previously, membrane enrichment with 0.5% GO additive caused the formation of closed pores, and this was the reason for the worst dye transport. In comparison to the pure PVDF membrane, the addition of 2% GO did not improve its transport properties, as confirmed by diagram b in Figure 7.

The effect of the GO content and the technique by which the membranes were formed on the water flux are shown in Figure 8. For all of the membranes formed by solvent evaporation, the pure water flux value was significantly lower in comparison to the membranes formed by coagulation. The value of the pure water flux depended on several factors, that is, the porosity and the pore size of the membranes.[9,25] The high value of the pure water flux may have been due to the hydrophilic properties of the membrane itself. The increase in the number of oxygen-containing functional groups on the membrane surface may have intensified the water sorption and, as a consequence, enhanced the water transport through the membrane.[34] Thus, the evaporated membranes, with a sharply lower porosity and a lower surface hydrophilicity, were characterized by a lower pure water flux.

A very interesting dependence for the evaporated membranes was observed. In this case, despite the introduction of GO as an additive, a comparatively decreased contact angle was observed compared to the pure membrane. Nevertheless, its pure water flux was higher. Moreover, similar results were observed for dye transport and the membrane without the GO additive. This was attributed to the membrane thickness, although its porosity and mean pore size were comparable to those of the M-5 membrane. This membrane was thinner than all of the prepared membranes, and this had a significant influence on its permeability. Among the membranes enhanced with GO, the highest pure water flux was achieved for the membrane prepared with 0.5% GO. This was rather expected behavior; this membrane had the highest porosity and mean pore size, and as mentioned previously, these parameters had a strong influence on the pure water flux. When the GO content was above 0.5%, the decrease in the pure water flux also reduced the porosity and mean pore size. The GO additive acted as a nucleating agent in the process of phase separation, speeding up and facilitating the membrane-

formation process. Nonetheless, when the amount of additive exceeded 0.5%, the viscosity of the casting solutions increased, and consequently, this slowed down the membrane-formation process. The resulting membrane was densely structured with a lower porosity and mean pore size.[25]

The water-coagulated membranes had the highest pure water flux when the GO was at a level of 1%. Through an analysis of the data in Table I, one can see that this membrane was characterized by the highest porosity and mean pore size. Similarly, as in the case of the evaporated membranes, when the threshold value of the GO content was exceeded, there were decreases in the porosity and mean pore size of the formed membranes. This threshold value for the coagulated membrane was slightly higher. An additive introduction level above 1% caused a reduction in the permeability.

CONCLUSIONS

The performed tests proved that among numerous factors influencing the PVDF membrane morphology and its properties, the formation technique and GO additives played crucial roles.

The membranes formed by coagulation in distilled water (technique 2) were characterized by noticeably better hydrophilic properties and a relatively higher porosity and permeability than the membranes obtained by solvent evaporation (technique 1).

The membranes with the most promising properties (i.e., porosity, thickness, transport properties) were those with a GO content of 0.5% obtained with technique 1 and those with a GO content of 1% obtained with technique 2.

On the basis of our research, we concluded that the optimal concentration of GO was 1%; above that level, there was no observed improvement in the physicochemical properties of the PVDF membranes.

REFERENCES

1. Kang, G.-D.; Cao, Y.-M. *J. Membr. Sci.* **2014**, *463*, 145.
2. Charcosset, C. *J. Food Eng.* **2009**, *92*, 241.
3. Zaviska, F.; Drogui, P.; Grasmick, A.; Azais, A.; Héran, M. *J. Membr. Sci.* **2013**, *429*, 121.
4. Ravanchi, M. T.; Kaghazchia, T.; Kargari, A. *Desalination* **2009**, *235*, 199.
5. Nataraj, S. K.; Sridhar, S.; Shaikha, I. N.; Reddy, D. S.; Aminabhavi, T. M. *Sep. Purif. Technol.* **2007**, *57*, 185.
6. Zhang, J.; Xu, Z.; Shan, M.; Zhou, B.; Li, Y.; Li, B.; Niu, J.; Qian, X. *J. Membr. Sci.* **2013**, *448*, 81.
7. Xia, S.; Ni, M. *J. Membr. Sci.* **2015**, *473*, 54.
8. Xu, H.-P.; Lang, W.-Z.; Zhang, X.; Guo, Y.-J. *J. Ind. Eng. Chem.* **2015**, *21*, 1005.
9. Zhao, Y.; Xu, Z.; Shan, M.; Min, C.; Zhou, B.; Li, Y.; Li, B.; Liu, L.; Qian, X. *Sep. Purif. Technol.* **2013**, *103*, 78.
10. Safarpour, M.; Khataee, A.; Vatanpour, V. *Sep. Purif Technol.* **2015**, *140*, 32.
11. Yeow, M. L.; Liu, Y. T.; Li, K. *J. Appl. Polym. Sci.* **2004**, *92*, 1782.
12. Liu, F.; Hashim, N. A.; Liu, Y.; Moghareh Abed, M. R.; Li, K. *J. Membr. Sci.* **2011**, *375*, 1.
13. Buonomenna, M. G.; Macchi, P.; Davoli, M.; Drioli, E. *Eur. Polym. J.* **2007**, *43*, 1557.
14. Zhao, C.; Xu, X.; Chen, J.; Yang, F. *Desalination* **2014**, *334*, 17.
15. Wang, Q.; Wang, Z.; Wu, Z. *Desalination* **2012**, *297*, 79.
16. Zhao, C.; Xu, X.; Chen, J.; Yang, F. *J. Environ. Chem. Eng.* **2013**, *1*, 349.
17. Cao, X.; Ma, J.; Shi, X.; Ren, Z. *Appl. Surf. Sci.* **2006**, *253*, 2003.
18. Wei, Y.; Chu, H. Q.; Dong, B. Z.; Li, X.; Xia, S. J.; Qiang, Z. M. *Desalination* **2011**, *272*, 90.
19. Liu, F.; Moghareh Abed, M. R.; Li, K. *J. Membr. Sci.* **2011**, *366*, 97.
20. Huang, Z. Q.; Zheng, F.; Zhang, Z.; Xu, H. T.; Zhou, K. M. *Desalination* **2012**, *292*, 64.
21. Yu, L. Y.; Xu, Z. L.; Shen, H. M.; Yang, H. *J. Membr. Sci.* **2009**, *337*, 257.
22. Ma, J.; Zhao, Y.; Xu, Z.; Min, C.; Zhou, B.; Li, Y.; Li, B.; Niu, J. *Desalination* **2013**, *320*, 1.
23. Zhao, C.; Xu, X.; Chen, J.; Wang, G.; Yang, F. *Desalination* **2014**, *340*, 59.
24. Ganesh, B. M.; Isloor, A. M.; Ismail, A. F. *Desalination* **2013**, *313*, 199.
25. Wang, Z.; Yu, H.; Xia, J.; Zhang, F.; Li, F.; Xia, Y.; Li, Y. *Desalination* **2012**, *299*, 50.
26. An, N.; Liu, S.; Fang, C.; Yu, R.; Zhou, X.; Cheng, Y. *J. Appl. Polym. Sci.* **2015**, *132*, 41577.
27. Konios, D.; Stylianakis, M. M.; Stratakis, E.; Kymakis, E. *J. Colloid Interface Sci.* **2014**, *430*, 108.
28. Hummers, W. S.; Offeman, R. E. *J. Am. Chem. Soc.* **1958**, *80*, 1339.
29. Zinadini, S.; Zinatizadeh, A. A.; Rahimi, M.; Vatanpour, V.; Zangeneh, H. *J. Membr. Sci.* **2014**, *453*, 292.
30. Fryczkowski, R.; Gorczowska, M.; Slusarczyk, C.; Fryczkowska, B.; Janicki, J. *Compos. Sci. Technol.* **2013**, *80*, 87.
31. Chen, J.; Yao, B.; Li, C.; Shi, G. *Carbon* **2013**, *64*, 225.
32. Chen, W.; Yan, L.; Bangal, P. R. *Carbon* **2010**, *48*, 1146.
33. El Achaby, M.; Arrakhiz, F. Z.; Vaudreuil, S.; Essassi, E. M.; Qaiss, A. *Appl. Surf. Sci.* **2012**, *258*, 7668.
34. Pezeshk, N.; Rana, D.; Narbaitz, R. M.; Matsuura, T. *J. Membr. Sci.* **2012**, *389*, 280.